Flicker Mitigation by Individual Pitch Control of Variable Speed Wind Turbines With DFIG

Yunqian Zhang, Zhe Chen, *Senior Member, IEEE*, Weihao Hu, *Member, IEEE*,
and Ming Cheng, *Senior Member, IEEE*

Abstract—Due to the wind speed variation, wind shear and tower shadow effects, grid connected wind turbines are the sources of power fluctuations which may produce flicker during continuous operation. This paper presents a model of an MW-level variable-speed wind turbine with a doubly fed induction generator to investigate the flicker emission and mitigation issues. An individual pitch control (IPC) strategy is proposed to reduce the flicker emission at different wind speed conditions. The IPC scheme is proposed and the individual pitch controller is designed according to the generator active power and the azimuth angle of the wind turbine. The simulations are performed on the NREL (National Renewable Energy Laboratory) 1.5-MW upwind reference wind turbine model. Simulation results show that damping the generator active power by IPC is an effective means for flicker mitigation of variable speed wind turbines during continuous operation.

Index Terms—Flicker, flicker mitigation, individual pitch control (IPC), variable speed wind turbine.

I. INTRODUCTION

DURING the last few decades, with the growing concerns about energy shortage and environmental pollution, great efforts have been taken around the world to implement renewable energy projects, especially wind power projects. With the increase of wind power penetration into the grid, the power quality becomes an important issue. One important aspect of power quality is flicker since it could become a limiting factor for integrating wind turbines into weak grids, and even into relatively strong grids if the wind power penetration levels are high [1].

Flicker is defined as "an impression of unsteadiness of visual sensation induced by a light stimulus, whose luminance or spectral distribution fluctuates with time" [2]. Flicker is induced by voltage fluctuations, which are caused by load flow changes in the grid. Grid-connected variable speed wind turbines are fluctuating power sources during continuous operation. The power fluctuations caused by wind speed variation, wind shear, tower shadow, yaw errors, etc., lead to the voltage fluctuations in the network, which may produce flicker [3]. Apart from the wind power source conditions, the power system characteristics also have impact on flicker emission of grid-connected wind turbines, such as short-circuit capacity and grid impedance angle [4], [5]. The flicker emission with different types of wind turbines is quite different. Though variable-speed wind turbines have better performance with regard to the flicker emission than fixed-speed wind turbines, with the large increase of wind power penetration level, the flicker study on variable speed wind turbines becomes necessary and imperative.

A number of solutions have been presented to mitigate the flicker emission of grid-connected wind turbines. The most commonly adopted technique is the reactive power compensation [6]. However, the flicker mitigation technique shows its limits in some distribution networks where the grid impedance angle is low [7]. When the wind speed is high and the grid impedance angle is $10°$, the reactive power needed for flicker mitigation is 3.26 per unit [8]. It is difficult for a grid-side converter (GSC) to generate this amount of reactive power, especially for the doubly fed induction generator (DFIG) system, of which the converter capacity is only around 0.3 per unit. The STATCOM which receives much attention is also adopted to reduce flicker emission. However, it is unlikely to be financially viable for distributed generation applications. Active power control by varying the dc-link voltage of the back-to-back converter is presented to attenuate the flicker emission [8]. However, a big dc-link capacitor is required, and the lifetime of the capacitor will be shortened to store of the fluctuation power in the dc link.

An open-loop pitch control is used in [6] and [8] to investigate the flicker emission in high wind speeds, however, the pitch actuation system (PAS) is not taken into account. Because the pitch rate and the time delay of the PAS make great contributions to the results of the flicker emission of variable-speed wind turbines, it is necessary to take these factors into consideration.

In recent years, IPC which is a promising way for loads reduction has been proposed [9]–[11], from which it is notable that the IPC for structural load reduction has little impact on the electrical power. However in this paper, an IPC scheme is proposed for flicker mitigation of grid-connected wind turbines. The power oscillations are attenuated by individual pitch angle adjustment according to the generator active power feedback and the wind turbine azimuth angle in such a way that the voltage fluctuations are smoothed prominently, leading to the flicker
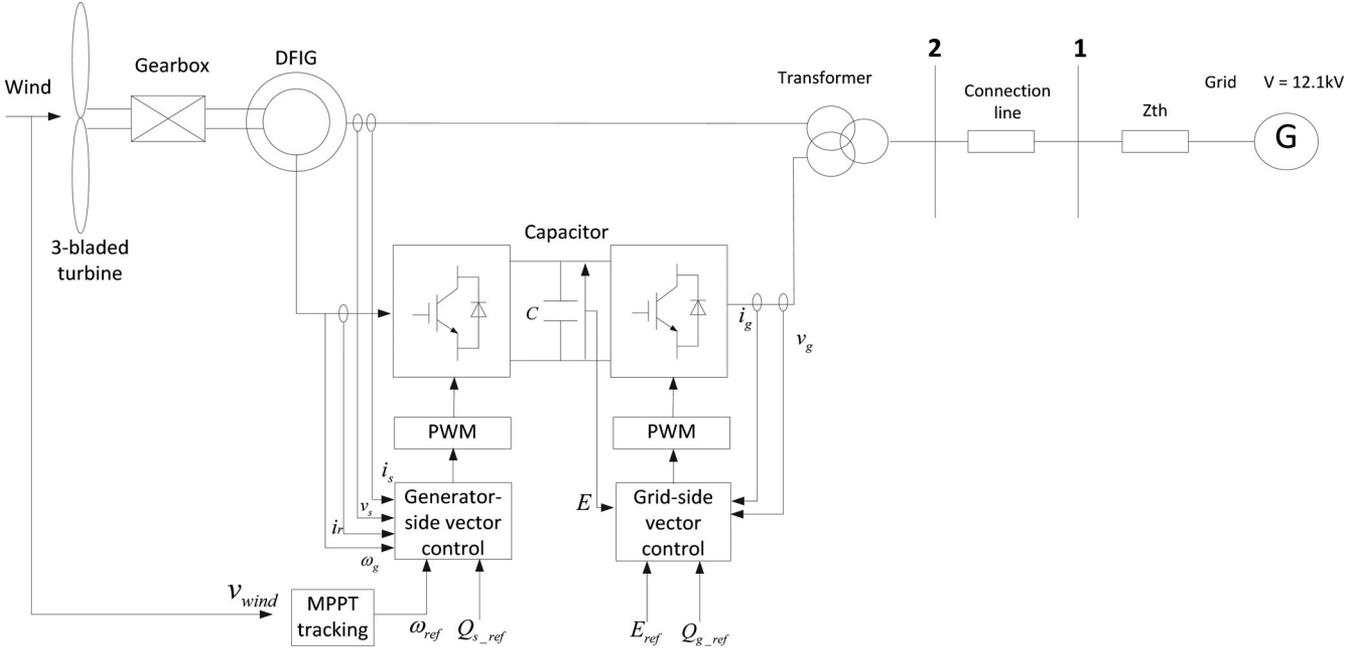
Fig. 1. Overall scheme of the DFIG-based wind turbine system.

mitigation. The influence of the flicker emission on the structural load is also investigated. The FAST (Fatigue, Aerodynamics, Structures, and Turbulence) code [12] which is capable of simulating three-bladed wind turbines is used in the simulation.

II. WIND TURBINE CONFIGURATION

The overall scheme of a DFIG-based wind turbine system is shown in Fig. 1, which consists of a wind turbine, gearbox, DFIG, a back-to-back converter which is composed of a rotor-side converter (RSC) and GSC, and a dc-link capacitor as energy storage placed between the two converters. In this paper, FAST is used to simulate the mechanical parts of wind turbine and the drivetrain. The pitch and converter controllers, DFIG, and power system are modeled by Simulink blocks.

A. FAST

The open source code FAST is developed at the National Renewable Energy Laboratory (NREL) and accessible and free to the public. FAST can be used to model both two and three bladed, horizontal-axis wind turbines. It uses Blade Element Momentum theory to calculate blade aerodynamic forces and uses an assumed approach to formulate the motion equations of the wind turbine. For three-bladed wind turbines, 24 degree of freedoms (DOFs) are used to describe the turbine dynamics. Their models include rigid parts and flexible parts. The rigid parts include earth, base plate, nacelle, generator, and hub. The flexible parts include blades, shaft, and tower. FAST runs significantly fast because of the use of the modal approach with fewer DOFs to describe the most important parts of turbine dynamics.

B. Mechanical Drivetrain

In order to take into account the effects of the generator and drivetrain on the wind turbine, two-mass model shown in Fig. 2
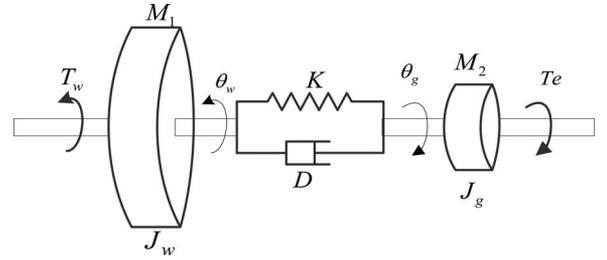

Fig. 2. Two-mass model of the drivetrain.

which is suitable for transient stability analysis is used [13]. The drivetrain modeling is implemented in FAST, and all values are referred to the wind turbine side.

The equations for modeling the drivetrain are given by

$$J_w \frac{d^2\theta_w}{dt^2} = T_w - D\left(\frac{d\theta_w}{dt} - \frac{d\theta_g}{dt}\right) - K(\theta_w - \theta_g) \quad (1)$$

$$J_g \frac{d^2\theta_g}{dt^2} = D\left(\frac{d\theta_w}{dt} - \frac{d\theta_g}{dt}\right) + K(\theta_w - \theta_g) - T_e \quad (2)$$

where J_w and J_g are the moment of inertia of wind turbine and generator, respectively, T_w, T_e are the wind turbine torque and generator electromagnetic torque, respectively, θ_w, θ_g are the mechanical angle of wind turbine and generator, K is the drivetrain torsional spring, D is the drivetrain torsional damper.

C. DFIG Model

The model of the DFIG is based on *dq* equivalent model shown in Fig. 3. All electrical variables are referred to the stator. u_{ds}, u_{qs}, u_{dr}, u_{qr}, i_{ds}, i_{qs}, i_{dr}, i_{qr} and ψ_{ds}, ψ_{qs}, ψ_{dr}, ψ_{qr} are the voltages, currents, and flux linkages of the stator and rotor in *d*- and *q*-axes, r_s and r_r are the resistances of the stator and rotor windings, L_s, L_r, L_m are the stator, rotor,
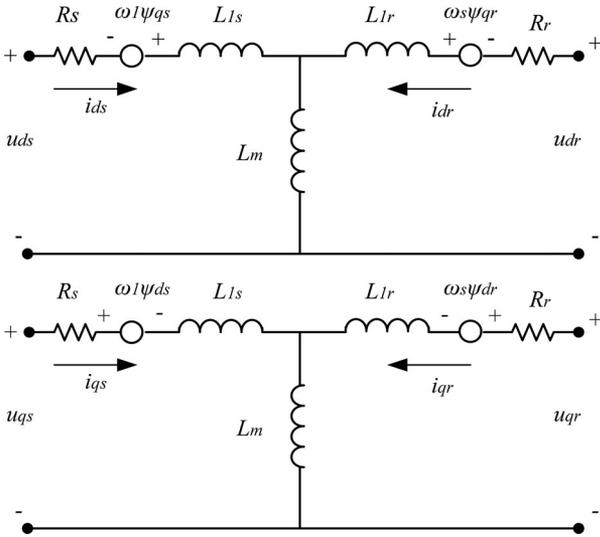
Fig. 3. $D - q$ equivalent circuit of DFIG at synchronously rotating reference frame.

and mutual inductances, L_{1s}, L_{1r} are the stator and rotor leakage inductances, w_1 is the speed of the reference frame, w_s is the slip angular electrical speed. The RSC of DFIG is controlled in a synchronously rotating d-q reference frame with the d-axis aligned along the stator flux position. The electrical torque T_e, active power P_s, and reactive power Q_s of DFIG can be expressed by [1]

$$T_e = \frac{3}{2}p\frac{L_m}{L_s}\psi_s i_{qr} \tag{3}$$

$$P_s = -\frac{3}{2}u_s\frac{L_m}{L_s}i_{qr} \tag{4}$$

$$Q_s = \frac{3}{2}\frac{\psi_s}{L_s}u_s - \frac{3}{2}u_s\frac{L_m}{L_s}i_{dr} \tag{5}$$

where p is the number of pole pairs, ψ_s is the stator flux, u_s is the magnitude of the stator phase voltage. From (4) and (5), due to the constant stator voltage, the active power and reactive power can be controlled via i_{qr} and i_{dr}.

III. WIND TURBINE CONTROL AND FLICKER EMISSION ANALYSIS

For a DFIG-based variable speed wind turbine, the control objective is different according to different wind speed. In low wind speed, the control goal is to keep the tip speed ratio optimum, so that the maximum power can be captured from the wind. In high wind speed, since the available power is beyond the wind turbine capacity, which could overload the system, the control objective is to keep the extracted power constant at its rated value.

A. Control of Back-to-Back Converter

Vector control techniques are the most commonly used methods for a back-to-back converter in a wind turbine system. Two vector control schemes are illustrated, respectively, for the RSC and GSC, as shown in Fig. 1, where v_s, and i_s are the stator
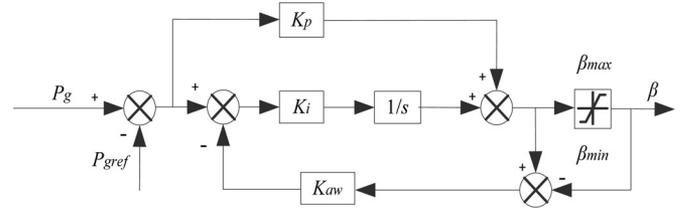

Fig. 4. PI controller with antiwindup.

voltage and current, i_r is the rotor current, v_g is the grid voltage, i_g is the GSC currents, w_g is the generator speed, E is the dc-link voltage, P_{s_ref}, and Q_{s_ref} are the reference values of the stator active and reactive power, Q_{r_ref} is the reference value of the reactive power flow between the grid and the GSC, E_{ref} is the reference value of the dc-link voltage, C is the dc-link capacitor. The vector control objective for RSC is to implement maximum power tracking from the wind by controlling the electrical torque of DFIG. The reference value of the generator speed ω_{ref} is obtained via a lookup table to enable the optimal tip speed ratio. The objective of GSC is to keep the dc-link voltage constant, while keeping sinusoidal grid currents. It may also be responsible for controlling the reactive power flow between the grid and the grid-side converter by adjusting Q_{g_ref}. Usually, the values of reactive power of RSC and GSC are set to zero to ensure unity power factor operation and reduce the current of RSC and GSC [1].

B. Pitch Control

Normally, pitch control is used to limit the aerodynamic power captured from the wind. In low wind speeds, the wind turbine should simply try to produce as much power as possible, so there is no need to pitch the blades. For wind speeds above the rated value, the pitch control scheme is responsible for limiting the output power.

The PI controller used for adjusting the pitch angles works well in normal operation, however, the performance of the pitch control system will degrade when a rapid change in wind speed from low to high wind speed is applied to the turbine rotor. It takes a long time for a positive power error contribution to cancel the effects of the negative pitch angle contribution that has been built up from integration of these negative power errors.

The integrator antiwindup scheme is implemented as shown in Fig. 4, in which the antiwindup term with gain K_{aw} is fed back to the integrator only. This prevents the integrated power error from accumulating when the rotor is operating in low wind speeds. The value for K_{aw} may be turbine dependent. When the pitch angle is not saturated, this antiwindup feedback term is zero [14].

C. Flicker Emission in Normal Operation

As discussed in Section I, flicker emission of a grid-connected wind turbine system is induced by voltage fluctuations which are caused by load flow changes in the network, so it is necessary to analyze the electrical power to the grid. Therefore, a simulation is conducted when the mean wind speed is 13 m/s
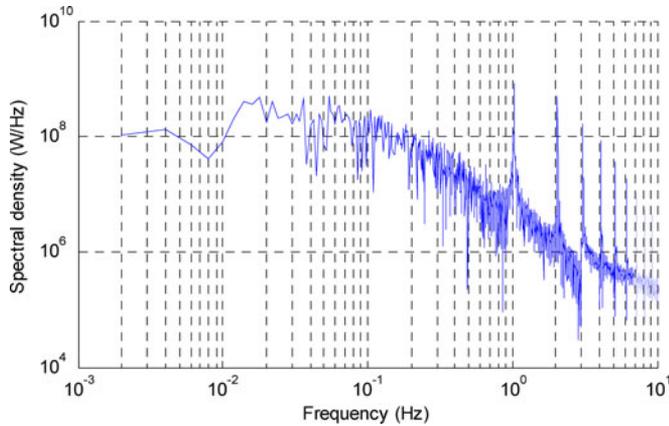
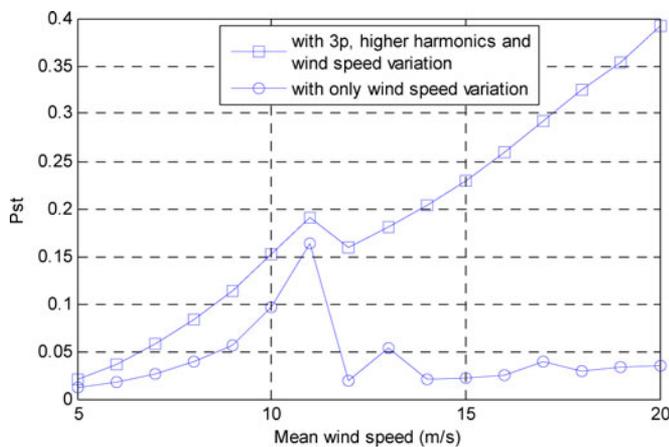Fig. 5.   Spectral density of the generator output power.

Fig. 6.   Flicker severity P_{st} between the cases with 3p, higher harmonics and wind speed variation (square), and the case with only wind speed variation (circle).

based on the model as shown in Fig. 1. The parameters of the wind turbine system are given in the Appendix. In this case, the turbine speed is around 0.345 Hz, which corresponds to the 3p frequency of 1.035 Hz, which is in conformation with the spectrum shown in Fig. 5. It is clearly seen that in addition to the 3p frequency, 6p, 9p, and higher frequencies are also included in the generator output power. These components will induce voltage fluctuations and flicker emission in the power grid.

Further, the flicker emission of a variable-speed wind turbine with DFIG is studied. The level of flicker is quantified by the short-term flicker severity P_{st}, which is normally measured over a 10-min period. According to IEC standard IEC 61000-4-15, a flickermeter model is adopted to calculate the short-term flicker severity P_{st} [6], [15], [16].

Fig. 6 illustrates the variation of flicker severity P_{st} with different mean wind speed between the cases with 3p, higher harmonics and wind speed variation and with only wind speed variation, respectively. In the first case, in low wind speeds, with the increase of mean wind speed the P_{st} increases accordingly, because higher mean wind speed with the same turbulence intensity means larger power oscillation and larger wind shear and tower shadow effects, leading to higher flicker severity. For

high wind speeds, where the wind turbine reaches rated power, the flicker level decreases due to the introduction of PI blade pitch control which could reduce the power oscillation in low frequency prominently, but it cannot effectively mitigate the power oscillations with 3p, 6p, 9p, and higher frequencies. As the power oscillation is bigger for higher wind speeds when the wind speed is above the rated wind speed, the flicker level continues to rise with the increase of mean wind speed.

In the case with only the wind speed variation, in low wind speeds the flicker emission has the similar situation, only the P_{st} is relatively smaller. In high wind speed, the P_{st} is much smaller, since the power oscillation contains little 3p and higher harmonics. From this figure, it can be concluded that the 3p and higher harmonics make a great contribution to the flicker emission of variable speed wind turbines with DFIG during continuous operation, especially in high wind speeds as shown in Fig. 6.

It is recommended that the flicker contribution from the wind farm at the point of common coupling shall be limited so that a flicker emission of P_{st} below 0.35 is considered acceptable [17]. From Fig. 6, it shows the maximum P_{st} is above 0.35 in this investigation where the turbulence intensity is 10%. As proved in [6], P_{st} will increase with the increase of the turbulence intensity; therefore, it is necessary to reduce the flicker emission. For this reason, a new control scheme for flicker mitigation by individual pitch control is proposed in next section.

IV. INDIVIDUAL PITCH CONTROL FOR FLICKER MITIGATION

This section concentrates on flicker mitigation of variable-speed wind turbines with DFIG during continuous operation using IPC.

The flicker emission produced by grid connected wind turbines during continuous operation is mainly caused by fluctuations in the generator active power. As illustrated in Fig. 6, the flicker emission will be mitigated effectively if the 3p and higher harmonics of the generator power can be reduced.

When the wind speed is above the rated wind speed, the pitch angle should be tuned by a traditional collective pitch control (CPC) to keep the output power at its rated value in order not to overload the system, and normally the 3p effect is not taken into consideration. For attenuating the generator power oscillation caused by the 3p effect, each of the three pitch angles can be added by a small pitch angle increment, which is dependent on the generator active power and wind turbine azimuth angle.

When the wind speed is below the rated wind speed, usually the control objective of the wind turbine is to implement maximum power tracking by generator electrical torque control. Pitch control is not used in this area. However if the pitch angles can be adjusted around a small average value, the 3p effect can also be reduced. For this purpose, the output of the CPC should leave a small amount of residual for pitch movement. This means a small part of wind energy will be lost.

Based on this concept, a novel IPC strategy is proposed. The control scheme is shown in Fig. 7. The control scheme consists of two control loops: CPC loop and IPC loop.
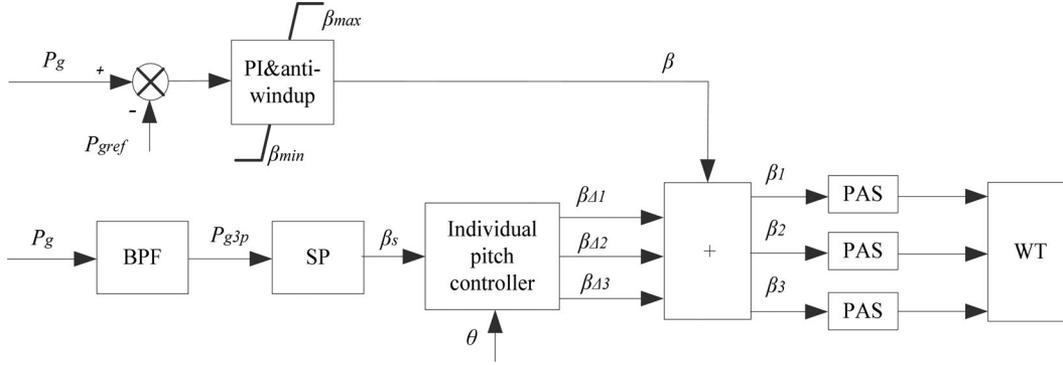
Fig. 7.   Proposed individual pitch control scheme.

The CPC loop is responsible for limiting the output power. In this loop, P_{g_ref} is the reference generator power which can be calculated according to different wind speed, P_g is the generator active power, β is the collective pitch angle, of which the minimum value $\beta_{\min}$ can be obtained by simulations under different wind speed such that the mitigation of generator power fluctuation should compromise the wind power loss. In the individual pitch control loop, the band pass filter (BPF) is to let the frequency of 3p generator active power P_{g3p} through and block all other frequencies. P_{g3p} is fed to the signal processing (SP) block, since the power signal has to be transferred to the pitch signal β_s which subsequently is passed to the individual pitch controller to output a pitch increment for a specific blade. The three pitch angles $\beta_{1,2,3}$ which are, respectively, the sum of collective pitch angles, and three pitch angle increments are sent to the PAS to adjust the three pitch angles to implement the mitigation of the generator active power oscillation.

A. Design of BPF

The transfer function of the BPF can be expressed as follows:

$$F(s) = \frac{Ks}{s^2 + (\omega_c/Q)s + \omega_c^2} \tag{6}$$

where ω_c is the center frequency, K is the gain, and Q is the quality factor.

ω_c which corresponds to the 3p frequency can be calculated by the measurement of the generator speed ω_g. $\omega_c = 3\omega_g/N$, where N is the gear ratio. The gain of the BPF at the center frequency is designed as 1 in order to let all the 3p frequencies pass the filter ($F(s) = KQ/\omega_c = 1$). Q which is responsible for the bandwidth of the BPF should be adjusted to let only the 3p component pass. In this case, Q is designed as $Q = \omega_c$.

Fig. 8 shows the Bode diagram of the BPF when the wind speed is above the rated value. In this case, the 3p frequency is 6.44 rad/s, and the bandwidth of the BPF which is around is 0.16 Hz (1 rad/s) is shown with the dotted lines.

B. Signal Processing

The SP block has to produce a pitch signal to offset the power oscillation, in such a way that the generator power will oscillate in a much smaller range.
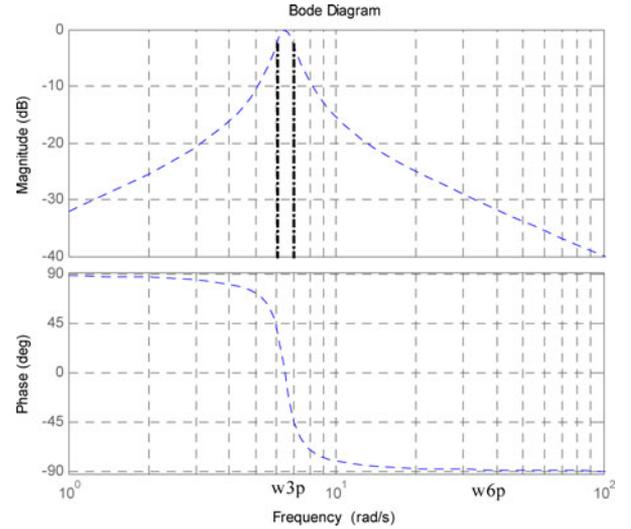

Fig. 8.   Bode diagram of the BPF (high wind speed).

Due to the time delay caused by the PAS and the power transfer from wind turbine rotor to the power grid, etc., the phase of the generator active power lags the phase of the pitch signal. In order to produce the correct phase angle shift of the SP block, it is very important to get the phase deviation of the component with 3p frequency of β and P_{g3p}. For this reason, the system is operated in high wind speed without the IPC loop. In this case, the collective pitch angle β contains the component with 3p frequency. The phase angle shift can be obtained by the component of β with 3p frequency and P_{g3p}.

The SP block can be implemented with a first-order lag element, which delays the phase angle at 3p frequency. The SP block can be represented as follows:

$$F_{sp}(s) = \frac{K_{sp}}{T_{sp}s + 1}. \tag{7}$$

The angular contribution of (7) is

$$\delta(\omega) = -\arctan(\omega T_{sp}). \tag{8}$$

Hence, the time constant T_{sp} can be calculated with the required angular contribution δ at ω_{3p}, shown as follows:

$$T_{sp} = -\frac{\tan \delta}{\omega_{3p}} \tag{9}$$

TABLE I
CONTROL PRINCIPLE OF INDIVIDUAL PITCH CONTROLLER

azimuth angle θ	β_s
$0 < \theta < 2\pi/3$	$\beta_{\Delta 2}$
$4\pi/3 > \theta > 2\pi/3$	$\beta_{\Delta 1}$
$2\pi > \theta > 4\pi/3$	$\beta_{\Delta 3}$

where ω_{3p} is the center frequency of the BPF.

The gain K_{sp} can be tuned by testing, as it has no contribution to the phase shift of the SP block. Increasing K_{sp} can accelerate the flicker mitigation; however, a big value of K_{sp} might increase the flicker emission of the wind turbine.

C. Individual Pitch Controller Design

The individual pitch controller will output the three pitch angle increments $\beta_{\Delta 1, \Delta 2, \Delta 3}$ for each blade based on the pitch signal β_s and the azimuth angle θ.

In this paper, the wind turbine is simulated by FAST, in which blade 3 is ahead of blade 2, which is ahead of blade 1, so that the order of blades passing through a given azimuth is 3–2–1-repeat. The individual pitch controller will output a pitch increment signal which will be added to the collective pitch angle for a specific blade, dependent on the blade azimuth angle. The principle of the individual pitch controller is described in Table I. For example, if the azimuth angle belongs to the area of $(0, 2\pi/3)$, then $\beta_{\Delta 2}$ equals β_s, and both $\beta_{\Delta 1}$ and $\beta_{\Delta 3}$ equal 0.

The three pitch increments will be, respectively, added with the collective pitch angle to give three total pitch angle demands. The three pitch angle signals will be sent to the PAS. The PAS can be represented using a first-order transfer function:

$$F(s) = \frac{1}{T_{\mathrm{pas}} s + 1} \qquad (10)$$

where T_{pas} which is a turbine dependent time constant of the PAS. In this case $T_{\mathrm{pas}} = 0.1$.

The control scheme shown in Fig. 7 is used for mitigation of the 3p component of the generator active power, leading to the reduction of the flicker emission which is caused by the 3p effect. Similar method can also be used to reduce the 6p component of the generator active power. However, this 6p component mitigation needs a much faster pitch actuation rate, which is not taken into account in this paper.

V. SIMULATION STUDIES USING IPC

The flicker mitigation using IPC is tested in many wind speed conditions. The variable speed wind turbine with DFIG and back-to-back converter are simulated with the proposed IPC method. The parameters of NREL 1.5-MW wind turbine with DFIG are shown in the Appendix.

Figs. 9 and 10 illustrate the short-term view and long-term view of the generator active power as well as the three pitch angles when the mean wind speed is above the rated wind speed. From these figures, it is shown that the generator active power to the grid is smoothed prominently. It is noted that when a power
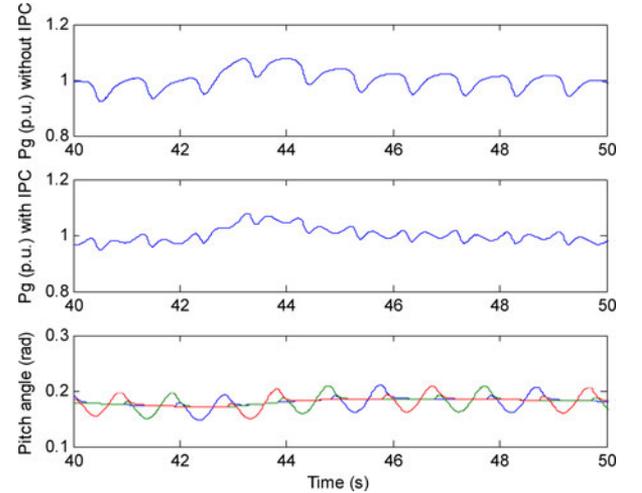

Fig. 9. Short-term view of the generator active power without and with IPC, and individual pitch angles (high wind speed).
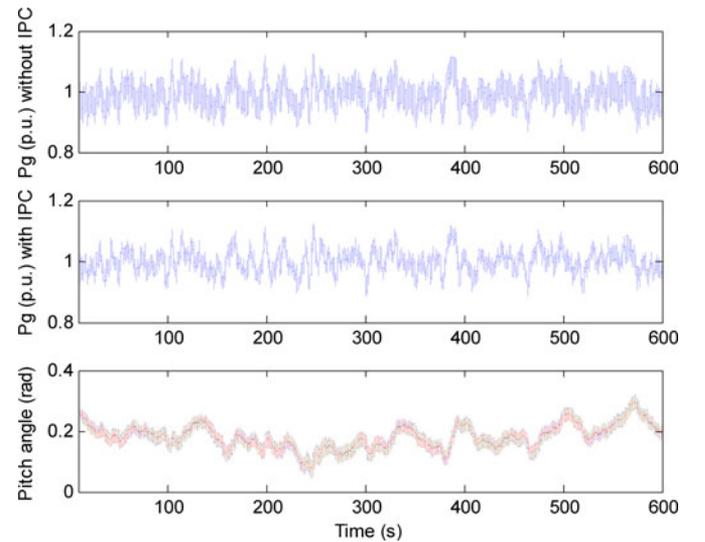

Fig. 10. Long-term view of the generator active power without and with IPC, and pitch angle (high wind speed).

drop occurs which is caused by wind shear, tower shadow, and wind speed variation, etc., one of the blades will accordingly reduce its pitch angle, thus the generator active power will not drop so dramatically, in such a way that the power oscillation is limited in a much smaller range.

A spectral density analysis of the generator active power into the grid has been conducted with IPC, as shown in Fig. 11. Compared with the spectral density of generator active power without IPC in Fig. 5, the 3p oscillation frequency component which is significant in flicker emission of variable speed wind turbines during continuous operation is damped evidently with IPC. As a consequence, the flicker level may be reduced by using IPC.

The wind turbine system employing IPC is also carried out when the mean wind speed is below the rated wind speed, as shown in Fig. 12. As a small pitch angle movement will contribute to high power variation, in this case, the minimum pitch
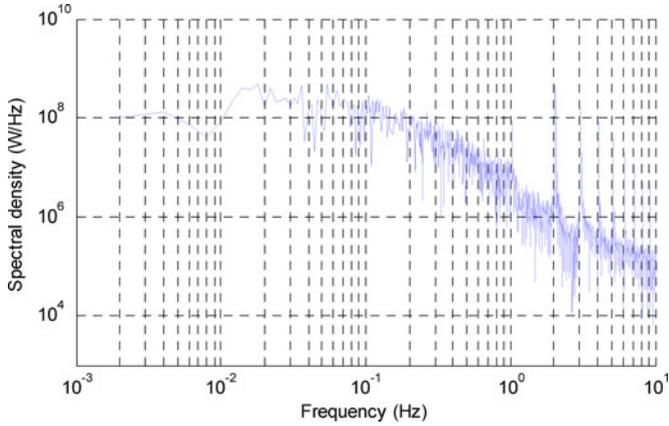
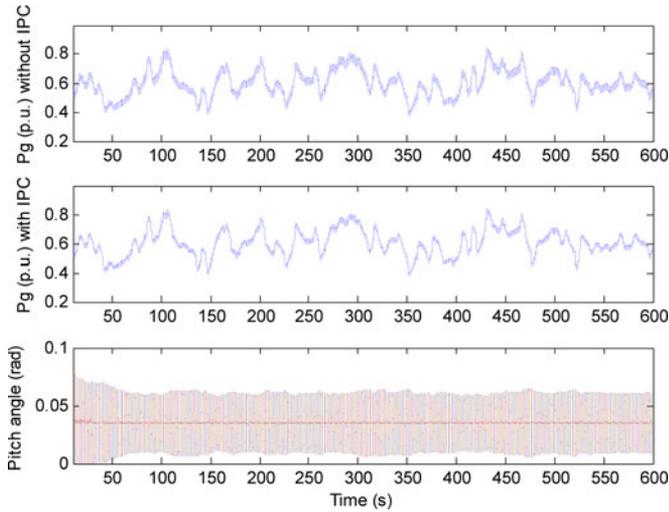Fig. 11.   Spectral density of the generator active power.

Fig. 12.   Long-term view of the generator active power without and with IPC, and pitch angle (low wind speed).

angle $\beta_{\min}$ in the CPC loop is set to 2° (0.0349 rad), leaving a small amount of residual for IPC to mitigate the power oscillation. The performance of the generator active power in Fig. 12 demonstrates that the IPC also works well in low wind speeds at the cost of some power loss due to the pitch movement.

Fig. 13 illustrates the variation of short-term flicker severity P_{st} with different mean wind speed between the case without IPC and the case with IPC. It can be concluded that damping the active power oscillation by using IPC is an effective means for flicker mitigation of variable speed wind turbines during continuous operation at different wind speed.

Since many IPC algorithms can mitigate the wind turbine loads [9]–[11], the proposed new IPC which can mitigate the flicker emission might have some impact on the wind turbine load. Therefore, the spectra of the blade root bending moment of blade 1 without and with IPC are plotted, respectively, in Fig. 14, which obviously shows that the load on the blade consists of 1p, 2p, 3p, and higher harmonics, and it demonstrates that the proposed IPC has little impact on the blade root bending moment. Due to the relationship between the rotor tilt and yaw moments and the blade root bending moments [9], it can also be
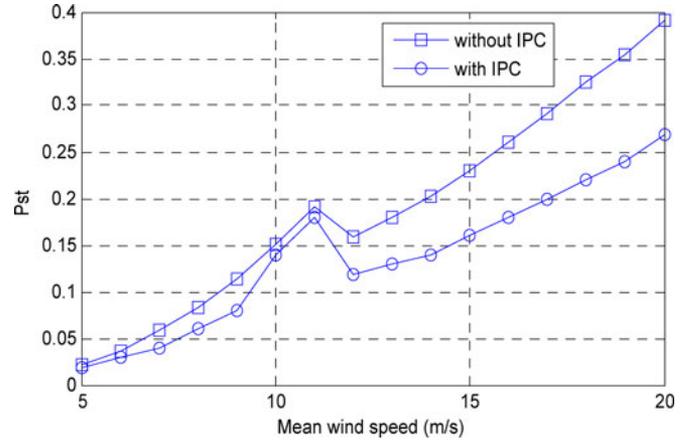

Fig. 13.   Flicker severity P_{st} between the case without IPC (square), and the case with IPC (circle).
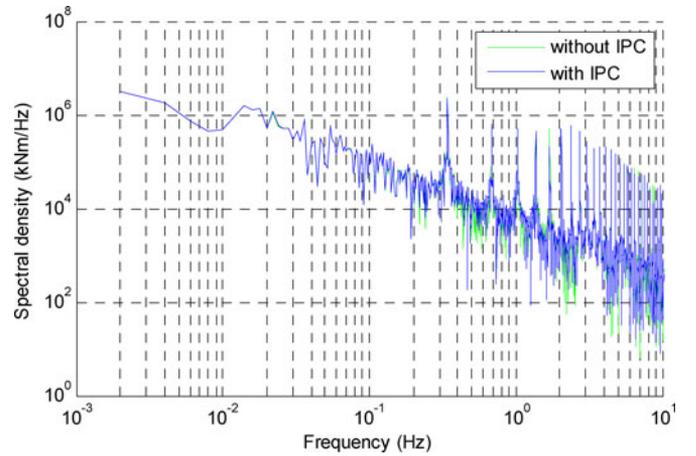
Fig. 14.   Spectra of the blade root bending moment.

Fig. 15.   Spectra of the wind turbine mechanical torque.

inferred that the proposed IPC has little impact on the tilt and yaw loads.

The mechanical torque of the wind turbine by using the proposed IPC is illustrated in Fig. 15, showing that compared with previous flicker emission methods [6]–[8], the 3p component of the mechanical torque is much reduced by using the presented

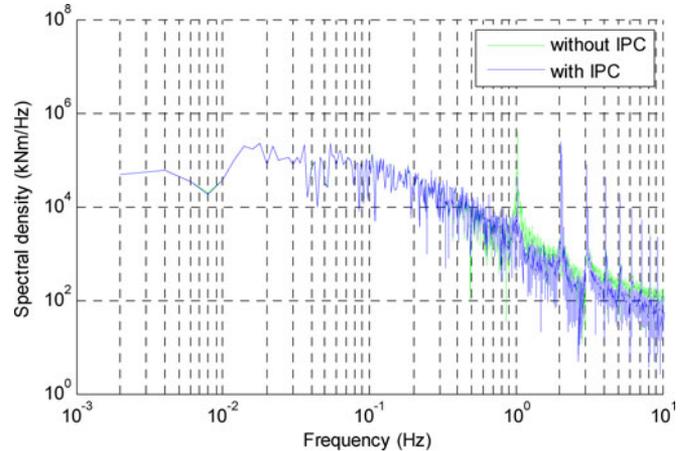IPC algorithm. As a consequence, the fatigue load of the wind turbine rotor is relatively smaller in comparison with the previous flicker mitigation methods, leading to the lifetime increase of the drive train.

There are also drawbacks of the proposed IPC method, such as loss of a small amount of wind energy in low wind speed and high demand of the PAS.

There is an alternative flicker mitigation method, which is the turbine rotor speed control taking advantage of the large rotor inertia. In this way, the wind power fluctuations can be stored in the wind turbine rotor, leading to the flicker mitigation. However, this paper is focused on the IPC method.

The IPC method for flicker mitigation proposed in this paper may be equally applicable to other types of variable speed wind turbines, such as a permanent magnet synchronous generator or a doubly salient permanent magnet generator, etc.

VI. Conclusion

This paper describes a method of flicker mitigation by IPC of variable-speed wind turbines with MW-level DFIG. The modeling of the wind turbine system is carried out using FAST and Simulink. On the basis of the presented model, flicker emission is analyzed and investigated in different mean wind speeds. To reduce the flicker emission, a novel control scheme by IPC is proposed. The generator active power oscillation which leads to flicker emission is damped prominently by the IPC in both high and low wind speeds. It can be concluded from the simulation results that damping the generator active power oscillation by IPC is an effective means for flicker mitigation of variable speed wind turbines during continuous operation.

Appendix
Parameters of the Wind Turbine With DFIG

DFIG and Wind turbine	
Rated capacity (MW)	1.5
Rated stator voltage(V)	690
Rated frequency(Hz)	50
Stator resistance(pu)	0.022
Rotor resistance(pu)	0.026
Stator leakage inductance(pu)	0.177
Rotor leakage inductance(pu)	0.116
Magnetizing inductance	4.68
Number of pole pairs	2
Lumped inertia constant(s)	3.0
Blade radius(m)	35
Number of blades	3
Gearbox ratio	81
Drivetrain torsional spring (Nm/rad)	5.6e9
Drivetrain torsional damper (Nm/s)	1.0e7
Hub height(m)	82.39
Rated power (MW) of wind turbine	1.5
Max/min pitch angle (degree)	45/0
Max pitch rate (degree/s)	10
Time constant of PAS	0.1
Turbulence intensity	10%
Impedance magnitude of line 1-2 (Ω)	0.7642
Short circuit capacity ratio	10
Short circuit impedance	1.5125+j2.619
Grid impedance angle (degree)	60

References

[1] T. Sun, "Power Quality of grid-connected wind turbines with DFIG and their interaction with the grid," Ph.D. dissertation, Aalborg Univ., Aalborg, Denmark, 2004.

[2] L. Rossetto, P. Tenti, and A. Zuccato, "Electromagnetic compatibility issues in industrial equipment," *IEEE Ind. Appl. Mag.*, vol. 5, no. 6, pp. 34–46, Nov./Dec. 1999.

[3] Å. Larsson, "Flicker emission of wind turbines during continuous operation," *IEEE Trans. Energy Convers.*, vol. 17, no. 1, pp. 114–118, Mar. 2002.

[4] H. Sharma, S. Islam, T. Pryor, and C. V. Nayar, "Power quality issues in a wind turbine driven induction generator and diesel hybrid autonomous grid," *J. Elect. Electron. Eng.*, vol. 21, no. 1, pp. 19–25, 2001.

[5] M. P. Papadopoulos, S. A. Papathanassiou, S. T. Tentzerakis, and N. G. Boulaxis, "Investigation of the flicker emission by grid connected wind turbines," in *Proc. 8th Int. Conf. Harmonics Quality Power*, Athens, Greece, 1998, vol. 2, pp. 1152–1157.

[6] T. Sun, Z. Chen, and F. Blaabjerg, "Flicker study on variable speed wind turbines with doubly fed induction generators," *IEEE Trans. Energy Convers.*, vol. 20, no. 4, pp. 896–905, Dec. 2005.

[7] K. Yun-Seong and W. Dong-Jun, "Mitigation of the flicker level of a DFIG using power factor angle control," *IEEE Trans. Power Del.*, vol. 24, no. 4, pp. 2457–2458, Oct. 2009.

[8] W. Hu, Z. Chen, Y. Wang, and Z. Wang, "Flicker mitigation by active power control of variable-speed wind turbines with full-scale back-to-back power converters," *IEEE Trans. Energy Convers.*, vol. 24, no. 3, pp. 640–649, Sep. 2009.

[9] E. A. Bossanyi, "Individual blade pitch control for load reduction," *Wind Energy*, vol. 6, pp. 119–128, 2002.

[10] E. A. Bossanyi, "Further load reductions with individual pitch control," *Wind Energy*, vol. 8, pp. 481–485, 2005.

[11] Y. Zhang, Z. Chen, M. Cheng, and J. Zhang, "Mitigation of fatigue loads using individual pitch control of wind turbines based on FAST," in *Proc. 46th Int. Conf. Universities' Power Eng.*, Soest, Germany, 2011.

[12] B. J. Jonkman and M. L. J. Buhl, "FAST User's Guide," National Renewable Energy Laboratory (NREL), Golden, CO, USA, Tech. Rep. NREL/EL-500-38230, (2005). [Online]. Available: http://wind.nrel.gov/designcodes/simulators/fast/

[13] S. M. Muyeen, M. Hasan, R. Takahashi, T. Murata, J. Tamura, Y. Tomaki, A. Sakahara, and E. Sasano, "Comparative study on transient stability analysis of wind turbine generator system using different drive train models," *IET Renewable Power Generation*, vol. 1, no. 2, pp. 131–141, 2007.

[14] A. D. Wright and L. J. Fingersh, "Advanced control design for wind turbines—Part I: Control design, implementation, and initial tests," National Renewable Energy Laboratory, NREL Rep. TP-500–42437, National Renewable Energy Laboratory, Mar. 2008.

[15] *Electromagnetic Compatibility (EMC)—Part 4: Testing and Measurement Techniques—Section 15: Flickermeter—Functional and Design Specifications*, IEC Std. 61 000–4–15, Nov. 1997.

[16] Å. Larsson, "Flicker emission of wind turbines during continuous operation," *IEEE Trans. Energy Convers.*, vol. 17, no. 1, pp. 114–118, Mar. 2002.

[17] *Grid Code 3.2.5 Wind Power Plant above 11 kW*. [Online]. Available:http://energinet.dk/

Yunqian Zhang received the B.Eng. and M.Sc. degrees from Anhui University of Science and Technology, Anhui, China, in 2004 and 2007, respectively, both in electrical engineering, and the Ph.D. degree from Aalborg University, Aalborg, Denmark, in 2013.

He is currently a Research Assistant at the Department of Energy Technology, Aalborg University. His research interests include wind turbine control and motor drives.

Zhe Chen (M'95–SM'98) received the B.Eng. and M.Sc. degrees from the Northeast China Institute of Electric Power Engineering, Jilin, China, and the Ph.D. degree from University of Durham, U.K.

He is a full Professor with the Department of Energy Technology, Aalborg University, Aalborg, Denmark. He is the Leader of Wind Power System Research program at the Department of Energy Technology, Aalborg University, and the Danish Principle Investigator for *Wind Energy* of *Sino-Danish Centre for Education and Research*. He has led many research projects and has more than 360 publications in his technical field. His research areas are power systems, power electronics, and electric machines, and his main current research interests include wind energy and modern power systems.

Dr Chen is an Editor of the IEEE TRANSACTIONS ON POWER SYSTEMS, an Associate Editor (Renewable Energy) of the IEEE TRANSACTIONS ON POWER ELECTRONICS, a Fellow of the Institution of Engineering and Technology (London, U.K.), and a Chartered Engineer in the U.K.

Ming Cheng (M'01–SM'02) received the B.Sc. and M.Sc. degrees from the Department of Electrical Engineering, Southeast University, Nanjing, China, in 1982 and 1987, respectively, and the Ph.D. degree from the Department of Electrical and Electronic Engineering, the University of Hong Kong, Hong Kong, in 2001.

Since 1987, he has been with Southeast University, where he is currently a Professor in the School of Electrical Engineering, the Director of the Research Center for Wind Power Generation and Associate Director of Yancheng Research Institute of New Energy Vehicle. As a Visiting Professor, he worked in WEMPEC, the University of Wisconsin-Madison from January to April, 2011, and in the Department of Energy Technology, Aalborg University, Denmark from June to July, 2012, respectively. He has authored or coauthored more than 300 technical papers and 5 books, and holds more than 50 patents in these areas. His teaching and research interests include electrical machines, motor drives for electric vehicles, and renewable energy generation.

Dr. Cheng received the "IET Premium Award in Electric Power Application," "GM Automotive Innovative Talent Award for China University," "SAE Environmental Excellence in Transportation Award-Education, Training and Public Awareness," and "Delta Scholar." He is a fellow of the Institution of Engineering and Technology. He has served as a Chair and organizing committee member for many international conferences.

Weihao Hu (S'06–M'13) received the B.Eng. and M.Sc. degrees from Xi'an Jiaotong University, Xi'an, China, in 2004 and 2007, respectively, both in electrical engineering, and the Ph.D. degree from Aalborg University, Aalborg, Denmark, in 2012.

He is currently a Postdoctoral Researcher at the Department of Energy Technology, Aalborg University. His research interests include smart grid, wind power generation, and electricity markets.